Human RNF169 is a negative regulator of the ubiquitin-dependent response to DNA double-strand breaks

Maria Poulsen,[1] Claudia Lukas,[2] Jiri Lukas,[2] Simon Bekker-Jensen,[1] and Niels Mailand[1]

[1]Ubiquitin Signaling Group, Department of Disease Biology, Novo Nordisk Foundation Center for Protein Research, Faculty of Health Sciences, University of Copenhagen, DK-2200 Copenhagen, Denmark
[2]Chromosome Biology Unit, Centre for Genotoxic Stress Research, Danish Cancer Society Research Center, DK-2100 Copenhagen, Denmark

Nonproteolytic ubiquitylation of chromatin surrounding deoxyribonucleic acid double-strand breaks (DSBs), mediated by the RNF8/RNF168 ubiquitin ligases, plays a key role in recruiting repair factors, including 53BP1 and BRCA1, to reestablish genome integrity. In this paper, we show that human RNF169, an uncharacterized E3 ubiquitin ligase paralogous to RNF168, accumulated in DSB repair foci through recognition of RNF168-catalyzed ubiquitylation products by its motif interacting with ubiquitin domain. Unexpectedly, RNF169 was dispensable for chromatin ubiquitylation and ubiquitin-dependent accumulation of repair factors at DSB sites. Instead, RNF169 functionally competed with 53BP1 and RAP80–BRCA1 for association with RNF168-modified chromatin independent of its catalytic activity, limiting the magnitude of their recruitment to DSB sites. By delaying accumulation of 53BP1 and RAP80 at damaged chromatin, RNF169 stimulated homologous recombination and restrained nonhomologous end joining, affecting cell survival after DSB infliction. Our results show that RNF169 functions in a noncanonical fashion to harness RNF168-mediated protein recruitment to DSB-containing chromatin, thereby contributing to regulation of DSB repair pathway utilization.

Introduction

Thousands of DNA-damaging insults are inflicted daily upon the genomes of all cells (Lindahl and Barnes, 2000). DNA double-strand breaks (DSBs) represent particularly cytotoxic lesions, which, if left unrepaired, may alter the content and organization of the genome (Wyman and Kanaar, 2006). To overcome this threat, cells have evolved a global DNA damage response, which impacts on diverse cellular processes, such as DNA repair, cell cycle progression, and transcription, to safeguard genome stability (Jackson and Bartek, 2009; Ciccia and Elledge, 2010). In response to DSBs, numerous signaling and repair proteins are recruited hierarchically to a protective microenvironment formed around lesions to facilitate efficient repair (Misteli and Soutoglou, 2009; Bekker-Jensen and Mailand, 2010). Protein assembly at such DSB repair foci is largely driven by posttranslational modifications of the DSB-flanking chromatin and attracted factors. Nonproteolytic ubiquitylation plays an important role in orchestrating protein retention at DSB repair foci, impinging on the ubiquitylation of histones and other proteins in the vicinity of DSBs to recruit DNA repair factors. Central to this process are the RNF8 and RNF168 ubiquitin ligases, which sequentially ubiquitylate the DSB-flanking chromatin to promote accumulation of DNA repair factors (Panier and Durocher, 2009; Bekker-Jensen and Mailand, 2010). Rapid recruitment of RNF8 to damaged chromatin triggers initial, Ubc13-dependent polyubiquitylation of H2A-type histones (Huen et al., 2007; Kolas et al., 2007; Mailand et al., 2007). This generates binding sites for the ubiquitin-binding motif interacting with ubiquitin (MIU) domains of RNF168, which amplifies nonproteolytic ubiquitylation of the DSB-associated chromatin to levels sufficient for allowing sustained retention of repair factors, such as BRCA1 and 53BP1 (Doil et al., 2009; Stewart et al., 2009). Recruitment of BRCA1 is mediated via RAP80, by means

Correspondence to Niels Mailand: niels.mailand@cpr.ku.dk

Abbreviations used in this paper: ATM, ataxia telangiectasia mutated; DR, direct repeat; DSB, double-strand break; HR, homologous recombination; IR, ionizing radiation; MIU, motif interacting with ubiquitin; NHEJ, nonhomologous end joining; WT, wild type.

The Rockefeller University Press $30.00
J. Cell Biol. Vol. 197 No. 2 189–199
www.jcb.org/cgi/doi/10.1083/jcb.201109100

of its tandem ubiquitin-interacting motifs that directly recognize RNF8/RNF168-catalyzed polyubiquitylated H2A species (Kim et al., 2007; Sobhian et al., 2007; Wang et al., 2007; Wu et al., 2009). How 53BP1 feeds on RNF8/RNF168-generated ubiquitin structures to accumulate at DSB sites is not fully understood but involves RNF8/RNF168-dependent removal of the H4K20me2-binding protein L3MBTL1 via p97/VCP to unblock 53BP1 binding sites (Acs et al., 2011).

Recent work has revealed that the DSB-responsive RNF8/RNF168-dependent chromatin ubiquitylation pathway is governed by a remarkable degree of regulatory complexity. A range of additional ubiquitin ligases accumulate in DSB repair foci, suggesting that many proteins at these structures are targeted by DSB-induced ubiquitylation (Bekker-Jensen and Mailand, 2010). Several negative regulators that restrain the magnitude and duration of the ubiquitin-dependent DSB response have also been identified. These include the deubiquitylating enzymes USP3, which removes ubiquitin from H2A- and H2B-type histones (Nicassio et al., 2007; Doil et al., 2009), and OTUB1, which suppresses the activity of the RNF168–Ubc13 complex independently of its catalytic activity (Nakada et al., 2010).

Most cellular DSBs are repaired by homologous recombination (HR) or nonhomologous end joining (NHEJ; Wyman and Kanaar, 2006). NHEJ, the predominant DSB repair pathway in mammalian cells, is operational at all stages of the cell cycle, but unlike HR, it is potentially error prone (Lieber, 2008). HR and NHEJ compete for repair of replication-associated DSBs, and maintaining a proper balance between these pathways may be critical for preserving genomic integrity (Sonoda et al., 2006; Shrivastav et al., 2008). The choice between NHEJ and HR is largely regulated at the level of 5′ end resection, an initial step in HR (San Filippo et al., 2008). Binding of 53BP1 to chromatid breaks during class switch recombination blocks their resection to suppress HR and promote NHEJ, and loss of 53BP1 in BRCA1-deficient cells rescues the HR defect observed in these cells (Bothmer et al., 2010; Bouwman et al., 2010; Bunting et al., 2010). Hence, the relative dynamics with which different DSB repair proteins accumulate at break sites may be an important aspect in determining the choice of DSB repair pathway for individual lesions.

Here, we identify human RNF169, an uncharacterized E3 ubiquitin ligase paralogous to RNF168, as a factor that negatively regulates the magnitude of the RNF8/RNF168-dependent signaling response to DSBs. Via its ubiquitin-binding MIU motif, RNF169 functionally competes with 53BP1 and RAP80–BRCA1 for recruitment to RNF168-modified chromatin at sites of DNA damage. Our findings show that ubiquitin ligases both positively and negatively regulate recruitment of repair factors to DSB sites to influence repair pathway utilization.

Results and discussion

RNF169 accumulates in DSB repair foci downstream of RNF8/RNF168

We noted that vertebrates encode an uncharacterized, apparent RNF168 paralogue known as RNF169/KIAA1991. Structurally, RNF169 resembles RNF168 in containing an N-terminal RING finger motif as well as a C-terminal putative MIU domain (Fig. 1 A; Penengo et al., 2006). Aside from these motifs, however, most of the intervening sequence of RNF168 and RNF169 do not align well, suggesting that they have nonredundant cellular functions. Because RNF168 is recruited to DSB repair foci by recognizing RNF8-dependent ubiquitylations via its MIU domains (Doil et al., 2009; Stewart et al., 2009), we speculated that RNF169 might accumulate in foci in a similar fashion. To test this, we assessed the subcellular distribution of RNF169. Throughout interphase, GFP-tagged RNF169 localized diffusely to the nucleoplasm in unperturbed cells but became concentrated in foci colocalizing with DSB markers, including γ-H2AX and MDC1, upon exposure to DSB-inducing agents, such as ionizing radiation (IR; Fig. 1 B and Fig. S1 A). Similarly, GFP-RNF169 was efficiently recruited to sites of microlaser-induced DSBs (Fig. 1 C). We raised RNF169 antibodies, but despite the fact that these detected endogenous RNF169 by immunoblotting (Fig. 1 D), they were not suitable for immunofluorescence, precluding us from assessing whether endogenous RNF169 is recruited to DSB repair foci. Using such antibodies, we found that RNF169 was expressed at a constant level throughout the cell cycle and that a substantial pool of RNF169 was associated with chromatin even in the absence of DNA damage (Fig. 1 D and Fig. S1, B and C).

To gain insight into the mechanism responsible for RNF169 accumulation in foci, we tested the impact of depleting known DSB-signaling factors. Knockdown of RNF8, HERC2, or RNF168 strongly suppressed the focal accumulation of RNF169 at DSB sites (Fig. 1 E), indicating that it required RNF8/RNF168-dependent ubiquitylation. Depletion of PIAS4, a SUMO (small ubiquitin-related modifier) E3 ligase required for RNF168 recruitment to DSBs (Galanty et al., 2009; Morris et al., 2009), also abolished RNF169 foci (Fig. 1 E). In contrast, knockdown of factors downstream of RNF8/RNF168 in the DSB-signaling pathway, including RAP80, BRCA1, and 53BP1, or inhibition of ataxia telangiectasia mutated (ATM) did not detectably impair the formation of IR-induced RNF169 foci (Fig. 1 E and Fig. S1 D). These observations suggest that RNF169 functions in the cellular response to DSBs downstream of RNF8/RNF168.

RNF169 is recruited to DSB sites via recognition of RNF168-dependent ubiquitin products

The potential ubiquitin-binding MIU domain in RNF169 and the requirement of RNF8/RNF168 for accumulation of RNF169 in DSB repair foci suggested that RNF169 might be recruited to these structures in a ubiquitin-dependent manner. To test this, we asked whether point mutations disrupting the functional integrity of the MIU (Fig. 2 A) or RING domains in RNF169 would impair its accumulation in foci. Whereas a catalytically inactive *RING mutant fully retained the ability to associate with DSB sites, mutation of the MIU domain rendered RNF169 completely deficient for such accumulation (Fig. 2, B and C). To corroborate this finding, we tested whether the MIU motif in RNF169 has ubiquitin-binding activity. Indeed, wild-type (WT), but not MIU-deficient, RNF169 bound efficiently to both

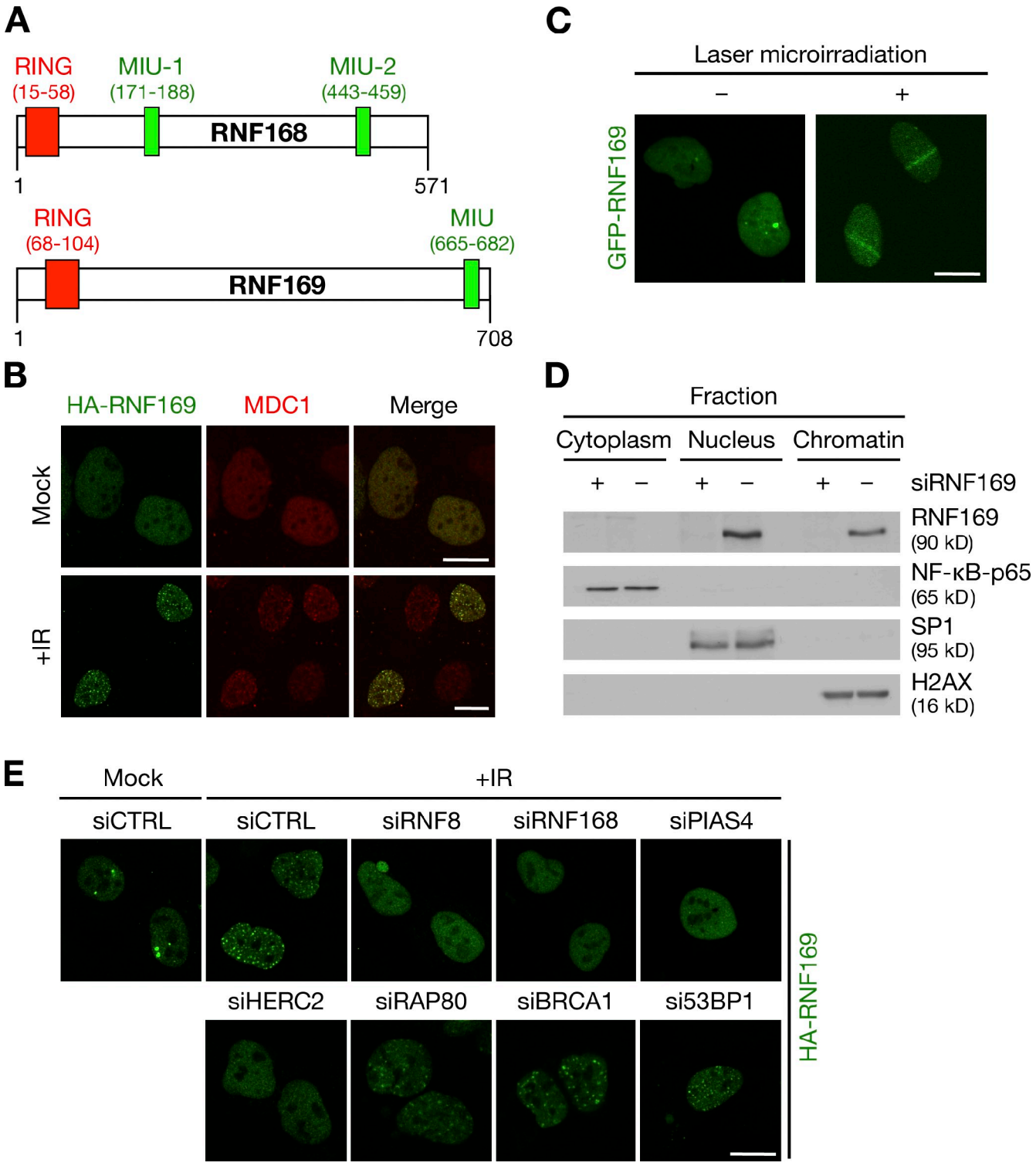

Figure 1. **RNF169 accumulates in DSB repair foci in an RNF8/RNF168-dependent manner.** (A) Schematic depiction of human RNF168 and RNF169 proteins, showing the location of conserved domains (amino acid residues are bracketed). (B) U2OS cells transiently transfected with the HA-RNF169 plasmid for 24 h were subjected or not subjected to IR (4 Gy), fixed 1 h later, and coimmunostained with HA and MDC1 antibodies. (C) U2OS cells stably expressing GFP-RNF169 were subjected or not subjected to microlaser irradiation and fixed 1 h later. (D) HeLa cells transfected or not transfected with RNF169 siRNA for 72 h were fractionated and immunoblotted with the indicated antibodies. (E) U2OS cells transfected with siRNAs for 48 h and with a HA-RNF169 plasmid for an additional 24 h were subjected or not subjected to IR (4 Gy), fixed 1 h later, and immunostained with the HA antibody. siCTRL, control siRNA. Bars, 10 µm.

K48- and K63-linked ubiquitin chains (Fig. 2 D). This suggests that the MIU motif is the predominant ubiquitin-binding module in RNF169, which may directly recognize RNF168-generated polyubiquitin structures at DSB sites. To test this, we reconstituted RNF168-depleted cells with siRNA-insensitive RNF168 WT or *RING alleles. Whereas RNF168 WT readily supported

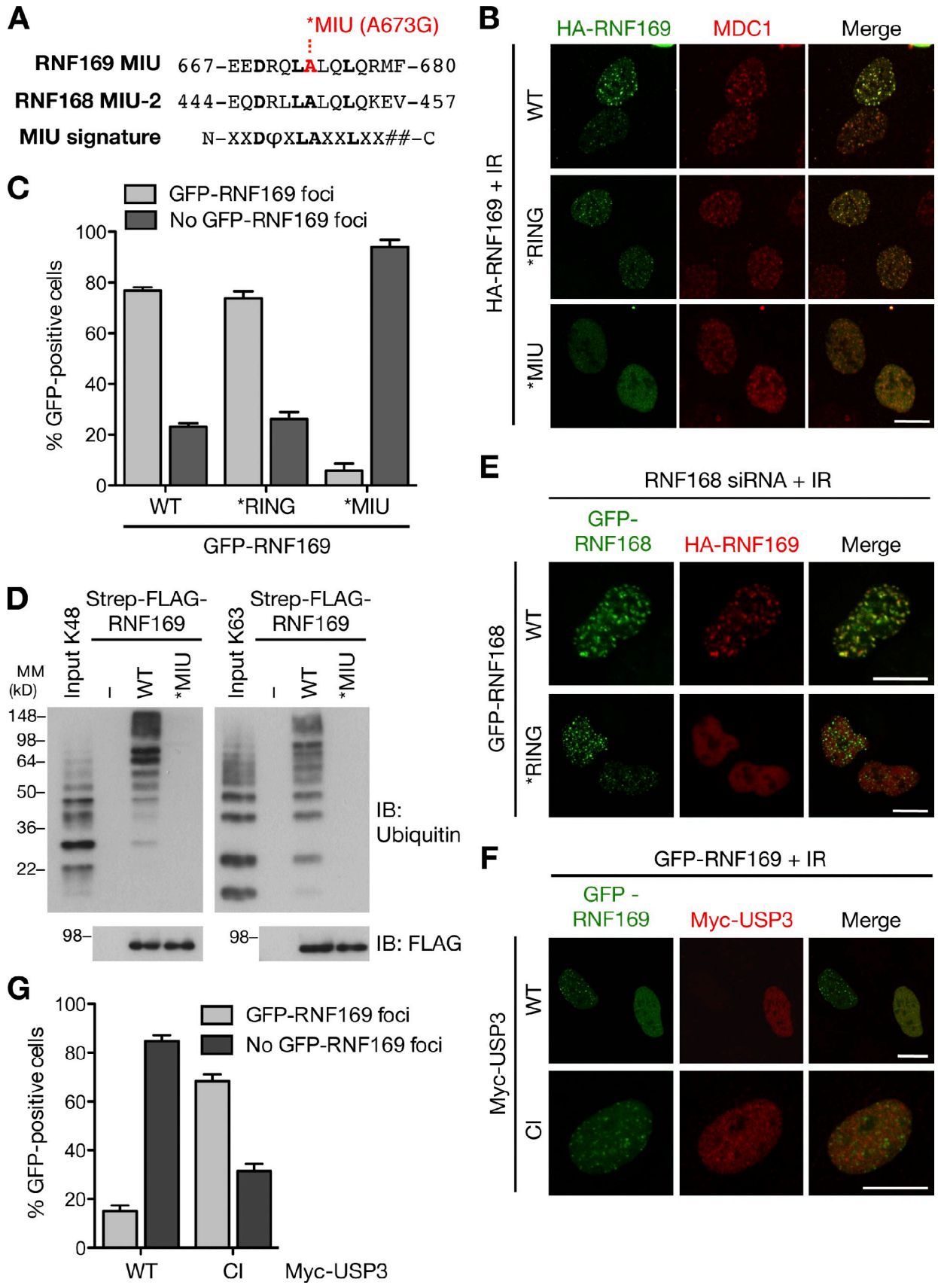

Figure 2. **RNF169 recognizes RNF168-catalyzed ubiquitin structures at DSB sites via its MIU domain.** (A) Alignment of the potential MIU motif in human RNF169 with human RNF168 MIU-2 and the signature MIU motif (Penengo et al., 2006). The RNF169 mutation disrupting the functional integrity of its MIU domain is indicated in red. Bold letters show residues of the MIU domain consensus motif. #, acidic residue; φ, large hydrophobic residue. N, N terminus; C, C terminus. (B) U2OS cells were transfected with the indicated HA-RNF169 constructs for 24 h, fixed, and immunostained

recruitment of RNF169 to DSB sites, cells expressing inactive RNF168 failed to do so (Fig. 2 E). Under these conditions, both WT and catalytically inactive RNF168 were recruited to DSB sites (Fig. 2 E), presumably through recognition of RNF8-catalyzed ubiquitylations. This indicates that, in contrast to its effect on RNF168, RNF8 is necessary, but not sufficient, to promote RNF169 retention at DSB-flanking chromatin. Consistently, we found that USP3, which deubiquitylates H2A-type histones to prevent accumulation of RNF168 and downstream repair factors, but not RNF8, at DSB sites (Nicassio et al., 2007; Doil et al., 2009), also suppressed RNF169 recruitment in a manner requiring its catalytic activity (Fig. 2, F and G). This further supports the notion that RNF169 recognizes factors directly modified by RNF168-mediated ubiquitylation in DSB repair foci via its MIU domain. Of note, association of RNF169 with nondamaged chromatin did not involve recognition of RNF8/RNF168-dependent ubiquitylations by the MIU domain (Fig. S1, E and F).

RNF169 is dispensable for ubiquitin-dependent protein assembly at DSB sites

The presence of RNF169 in DSB repair foci and its similarity to RNF168 prompted us to test whether RNF169 is required for ubiquitin-dependent protein recruitment to DSB sites. However, even in cells in which RNF169 expression was quantitatively reduced (Fig. 3 B), we found that, unlike RNF168, it was fully dispensable for accumulation of ubiquitin conjugates and repair factors, such as 53BP1, in foci (Fig. 3 A and Fig. S2 D). Consistently, despite the strong association of RNF169 with chromatin, it did not display appreciable E3 ligase activity toward H2A-type histones, the known target of the DSB-responsive RNF8/RNF168 ubiquitin ligase cascade, upon overexpression in cells (Fig. 3 C) or in in vitro ubiquitylation assays using purified proteins (Fig. 3 D). In contrast, in agreement with our previous findings (Doil et al., 2009), RNF168 catalyzed robust H2A polyubiquitylation under these conditions (Fig. 3, C and D). The inability of RNF169 to promote H2A ubiquitylation could not be explained by a general lack of RNF169 activity because purified RNF169 displayed clear autoubiquitylation activity in vitro (Fig. 3 E). By comparison, however, RNF168 was a much more potent E3 ligase than RNF169 (Fig. 3 E). Moreover, unlike RNF8 and RNF168, RNF169 did not detectably support Ubc13-associated ubiquitin ligase activity (unpublished data). We conclude from these experiments that despite being an active chromatin-bound E3 ubiquitin ligase, RNF169 is dispensable for ubiquitin-dependent protein assembly at DSB repair foci.

RNF169 competes with genome caretakers for ubiquitin-dependent recruitment to DSB repair foci

Because RNF169 recognizes RNF168-dependent polyubiquitin structures but does not appear to contribute to DSB-induced chromatin ubiquitylation, we reasoned that RNF169 might instead negatively regulate this pathway by competing with DSB repair factors for binding to damaged chromatin. Strikingly, in agreement with this hypothesis, elevated levels of ectopic RNF169 WT strongly impaired 53BP1 relocalization to DSB sites (Fig. 4, A and B). This did not require the catalytic activity of RNF169, as RNF169 *RING inhibited 53BP1 foci formation as efficiently as the WT protein (Fig. 4, A and B). In contrast, expression of the ubiquitin binding–deficient *MIU mutant did not interfere with 53BP1 recruitment to DSB sites (Fig. 4, A and B). Elevated levels of RNF169 also efficiently inhibited recruitment of RAP80 to damaged chromatin and reduced BRCA1 accumulation in microlaser tracks (Fig. 4 C and Fig. S2 A). The residual BRCA1 signal at the DSB-flanking chromatin most likely reflects its ability to associate with single-stranded DNA around DSBs independently of RAP80 as previously reported (Bekker-Jensen et al., 2006; Sobhian et al., 2007; Hu et al., 2011). These observations suggest that by recognizing RNF168-generated ubiquitylations, RNF169 functions in a noncatalytic manner to interfere with recruitment of genome caretaker factors to damaged chromatin. Consistently, RNF169 overexpression did not affect accumulation of γ-H2AX, RNF168, and conjugated ubiquitin species at DSB sites (Fig. 4 D and Fig. S2 B), further demonstrating that RNF169 only affects ubiquitin-dependent protein recruitment to DSB sites downstream of RNF168. To corroborate these findings, we monitored the impact of RNF169 knockdown on the magnitude of 53BP1 recruitment to DSB sites. We noted that siRNA-mediated depletion of RNF169 markedly enhanced the intensity of 53BP1 foci but not those of break-associated ubiquitin conjugates and RNF168 at early stages of the DSB response (Fig. 4 E and Fig. S2, C–E). We reasoned that this might result from loss of RNF169 binding to RNF168-generated polyubiquitin structures. To test in an unbiased fashion the impact of RNF169 removal on the magnitude of 53BP1 accrual, we performed automated analysis of the intensity of 53BP1 foci in a large cohort of RNF169-depleted cells. Whereas knockdown of RNF169 did not significantly alter the intensity of γ-H2AX foci, we noted a reproducible 1.5-fold increase in the mean intensity of 53BP1 foci (Table 1). These data support the notion that RNF169 functionally competes with DSB repair factors for ubiquitin-dependent recruitment to DSB sites and consequently dampens the magnitude of their accumulation at these structures.

with HA and MDC1 antibodies. (C) Quantification of data in B. At least 200 cells were counted for each treatment. (D) Lysates from HEK293T cells transfected with the indicated RNF169 expression plasmids or empty vector (−) for 24 h were subjected to Strep-Tactin pull-down under denaturing conditions, washed, and incubated with ubiquitin chains. Bound complexes were immunoblotted with ubiquitin and FLAG antibodies. (E) U2OS cells transfected with RNF168 siRNA for 48 h were transfected with siRNA-resistant GFP-RNF168 expression constructs for an additional 24 h and then subjected to IR (4 Gy) and fixed 1 h later. Cells were immunostained with the HA antibody. (F) U2OS cells cotransfected with GFP-RNF169 and WT or catalytically inactive (CI) Myc-USP3 constructs for 24 h were subjected to IR (4 Gy), fixed 1 h later, and immunostained with the Myc antibody. (G) Quantification of data in F. At least 200 cells were counted for each treatment. Results depict the means (±SD) of three independent experiments. IB, immunoblot; MM, molecular mass. Bars, 10 µm.

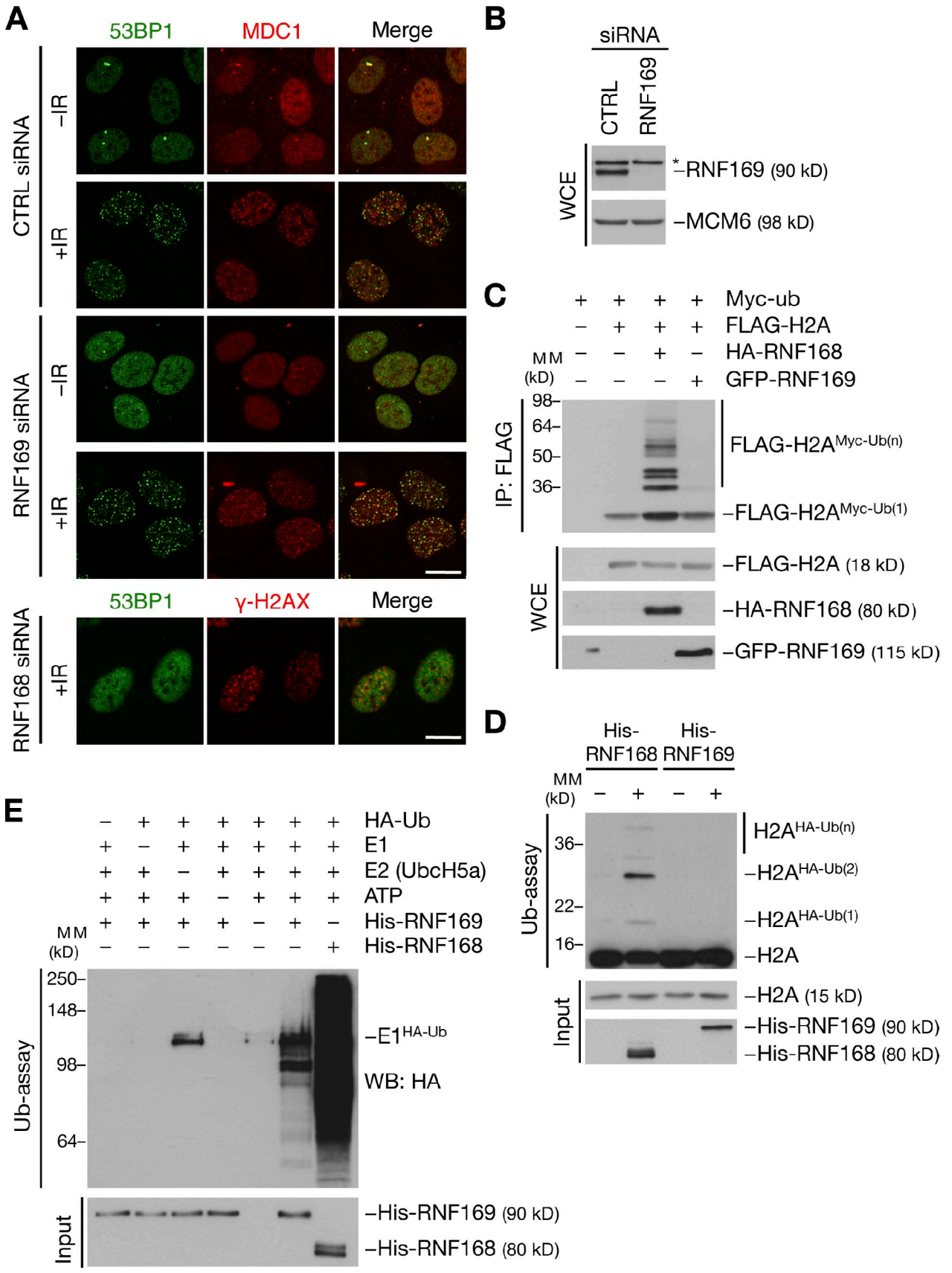

Figure 3. **RNF169 is dispensable for ubiquitin-dependent assembly of repair factors at DSB-modified chromatin.** (A) U2OS cells transfected with the indicated siRNAs for 72 h were subjected or not subjected to IR (4 Gy), fixed 1 h later, and coimmunostained with 53BP1 and MDC1 or γ-H2AX antibodies. Bars, 10 µm. (B) Immunoblot analysis of the experiment in A. The asterisk denotes a cross-reactive band. (C) HEK293T cells were transfected with the indicated combinations of plasmids for 24 h. To analyze histone H2A ubiquitylation, FLAG immunoprecipitates were immunoblotted with the Myc antibody.

The exact nature of the ubiquitylated species recognized by the MIU domain of RNF169 at DSB sites remains to be established. Because RNF169 limits both 53BP1 and RAP80 recruitment to RNF8/RNF168-ubiquitylated chromatin, these may include both ubiquitylated core histones, recognized by RAP80 (Wu et al., 2009), and the as yet unknown chromatin receptors for VCP/p97 that target it to DSBs to facilitate 53BP1 recruitment (Acs et al., 2011).

RNF169 regulates DSB repair pathway utilization

The impact of RNF169 on protein assembly dynamics at DSB sites suggested that it may play a role in regulating DSB repair pathway utilization. Indeed, we found that RNF169 depletion significantly decreased HR efficiency in cells, whereas knockdown of RNF168 had an opposite effect (Fig. 4 F). The reduced levels of HR in RNF169 siRNA-treated cells could be fully rescued by expression of ectopic RNF169 (Fig. S3 A). Consistently, overexpression of GFP-RNF169 WT, but not *MIU, stimulated HR efficiency (Fig. 4 G), and elevated levels of RNF169 negatively impacted on NHEJ (Fig. S3 B). Because both 53BP1 and RAP80 have recently been shown to suppress HR-mediated DSB repair (Bothmer et al., 2010; Coleman and Greenberg, 2011; Hu et al., 2011), these observations suggest that RNF169 facilitates DSB repair via HR by delaying and limiting the association of 53BP1 and RAP80 with ubiquitin-modified chromatin at DSBs.

The RNF8/RNF168 pathway promotes cell survival in response to DSBs (Panier and Durocher, 2009; Bekker-Jensen and Mailand, 2010). We used cell lines stably expressing different RNF169 alleles to test whether elevated levels of RNF169 compromised cell survival after DSB infliction. We found that ectopic RNF169 WT and *RING, but not the *MIU mutant, sensitized cells to IR to an extent comparable with that observed in RNF8- or RNF168-depleted cells (Fig. 4, H and I; and Fig. S3, C and D; Mailand et al., 2007; Doil et al., 2009). Although siRNA-mediated depletion of RNF169 reduced overall HR efficiency (Fig. 4 F), it did not manifest a significant effect on long-term cell survival in response to IR (Fig. S3 E).

In summary, our data demonstrate that human RNF169 is a novel ubiquitin ligase recruited to DSB-modified chromatin, further extending the spectrum of E3 ligases present in this locale. Despite the fact that RNF169 structurally resembles RNF168, it plays an unexpected role in restraining the magnitude of the RNF8/RNF168-dependent DSB response by functionally competing with 53BP1, RAP80–BRCA1, and possibly other factors for retention at damaged chromatin independently of its intrinsic E3 ligase activity. Hence, RNF169 provides the first example of a ubiquitin ligase that functions in a noncatalytic manner to negatively regulate the magnitude of protein accumulation at DSB-flanking chromatin, further broadening regulatory principles and complexity used in ubiquitin-dependent DSB signaling responses. The relative kinetics of assembly of different DNA repair factors at DSB sites may be important for determining the choice of repair mechanism. By competing with 53BP1 and RAP80 for binding to ubiquitin-modified chromatin near DSBs, RNF169 may function to limit the extent to which NHEJ, the predominant mode of DSB repair in mammalian cells, is used for lesion processing. This may be particularly important for channeling repair of replication-associated DSBs to the error-free HR pathway. Whether RNF169 has additional functions in chromatin maintenance remains to be established. Although purified RNF169 has inherent ubiquitin ligase activity, our data do not hint at an obvious function of this activity in promoting signaling responses to DSBs. We consider it likely, however, that RNF169 engages in other cellular processes that may involve its catalytic activity. Identification of the cellular RNF169 substrates should help to shed further light on the precise biological functions of this ubiquitin ligase.

Materials and methods

Plasmids and RNAi

Full-length human *RNF169* cDNA was amplified by PCR and inserted into pcDNA3 (Invitrogen) containing an N-terminal HA tag, pAcGFP-C1 (Takara Bio Inc.), and pcDNA4/TO (Invitrogen) containing an N-terminal S-FLAG-Strep tag to generate expression constructs for HA-, GFP-, and S-FLAG-Strep–tagged RNF169, respectively. pAcGFP-C1-RNF168 WT and *RING (C16S) constructs (Doil et al., 2009) were rendered insensitive to RNF168 siRNA by introducing the underlined silent mutations (5′-GAAGGCGGGCCAUGGAGGA-3′) into the RNF168 coding region. The pcDNA3-Myc-USP3 (WT and C168S mutated, catalytically inactive) expression plasmids were described previously (Doil et al., 2009). The *RING (C68S) and *MIU (A673G) point mutations in RNF169 constructs were introduced using the site directed mutagenesis kit (QuikChange; Agilent Technologies). All constructs were verified by sequencing. Plasmid transfections were performed using FuGENE 6 (Roche) according to the manufacturer's instructions. siRNA transfections were performed with transfection reagent (Lipofectamine RNAiMAX; Invitrogen) as described in this paper. siRNA target sequences used in this study were control,5′-GGGAUACCUAGACGUUCUA-3′;RNF169(#1),5′-GGUCCUCUCUGAGUAUACU-3′; RNF8, 5′-UGCGGAGUAUGAAUAUGAA-3′; RNF168, 5′-GGCGAAGAGCGAUGGAGGA-3′; PIAS4-1, 5′-GGAGUAAGAGUGGACUGAA-3′; HERC2, 5′-GGAUGAUCAUGAAGAGUUA-3′; RAP80, 5′-GGGUCCAAAAGUUGACAAA-3′; BRCA1, 5′-GAAACGGACUUGCUAUUUA-3′; 53BP1, 5′-GAACGAGGAGACGGUAAUA-3′; RAD51, 5′-GAGCUUGACAAACUACUUC-3′; and C-terminal–binding protein–interacting protein, 5′-GCUAAAACAGGAACGAAUC-3′.

Cell culture

Human U2OS, HeLa, and HEK293T cells were cultured in DME containing 10% fetal bovine serum. To generate cell lines stably expressing S-FLAG-Strep–tagged RNF169 WT, *RING, and *MIU alleles, U2OS cells were cotransfected with pcDNA6/TR (Invitrogen) and pcDNA4/TO-S-FLAG-Strep-RNF169 constructs, and positive clones were selected by incubation in medium containing 400 µg/ml Zeocin and 5 µg/ml Blasticidin S (both obtained from Invitrogen) for 14 d.

Immunochemical methods

Immunoblotting, immunoprecipitation, and Strep-Tactin pull-downs were performed as previously described (Mailand et al., 2006, 2007). In brief, cells were lysed in EBC buffer (50 mM Tris, pH 7.5, 150 mM NaCl, 1 mM EDTA, 1 mM DTT, and 0.5% NP-40) or denaturing buffer (20 mM Tris, pH 7.5, 50 mM NaCl, 1 mM EDTA, 1 mM DTT, 0.5% NP-40, 0.5% sodium deoxycholate, and 0.5% SDS) supplemented with protease and phosphatase

(D) Ubiquitylation reactions containing recombinant H2A, HA-ubiquitin, E1, and E2 (UbcH5a) were incubated in the presence or absence of purified His_6-RNF168 or His_6-RNF169 for 1 h and processed for immunoblotting with HA, H2A, and His_6 antibodies. (E) Reactions containing the indicated components were processed as in D and immunoblotted with the HA antibody to visualize RNF168 and RNF169 autoubiquitylation. CTRL, control; IP, immunoprecipitation; MM, molecular mass; Ub, ubiquitin; WCE, whole-cell extract; WB, Western blot.

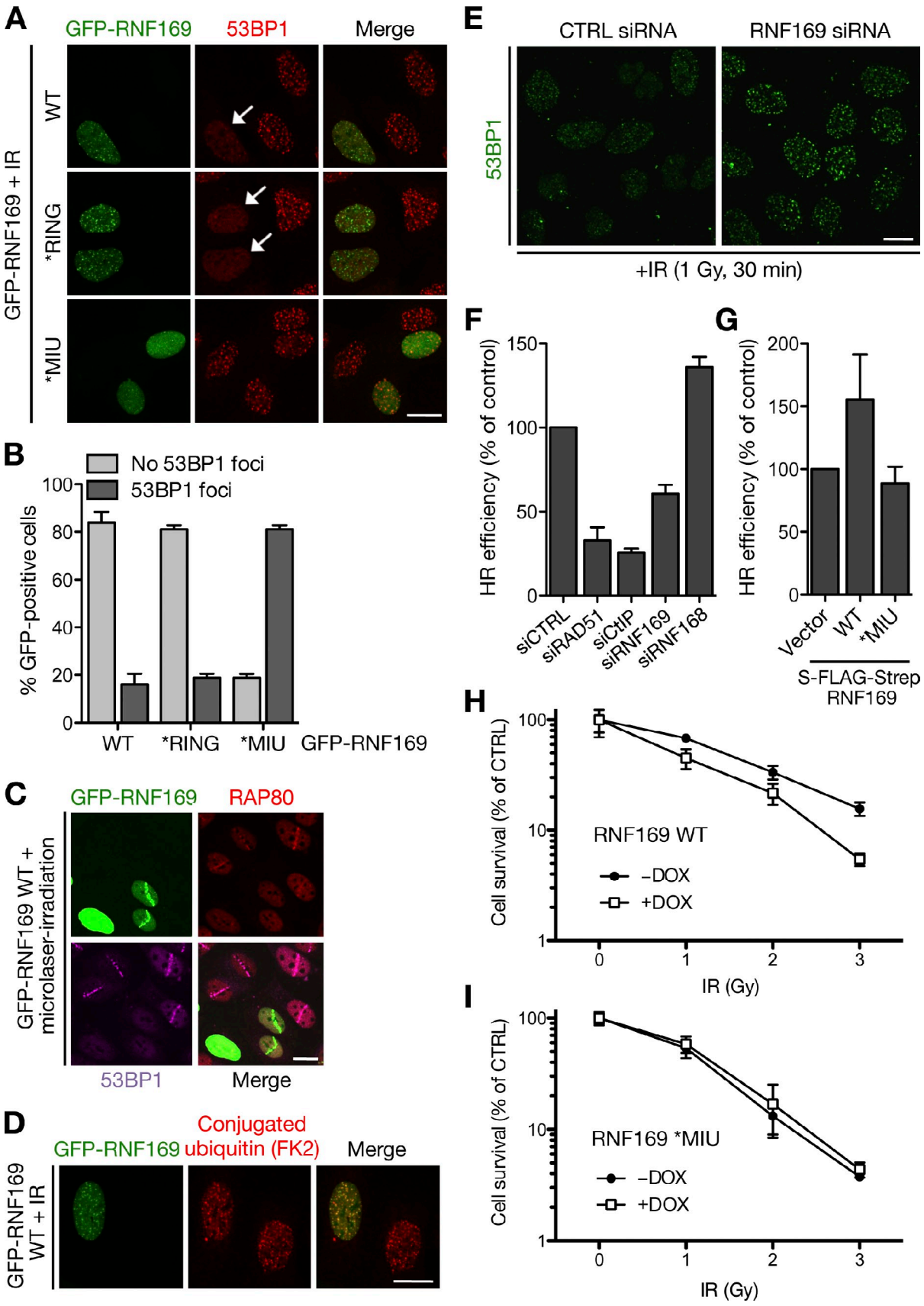

Figure 4. **RNF169 negatively regulates 53BP1 and RAP80 recruitment to DSBs to affect repair pathway choice.** (A) U2OS cells transfected with GFP-RNF169 expression plasmids for 24 h were exposed to IR (4 Gy), fixed 1 h later, and immunostained with the 53BP1 antibody. Arrows depict cells in which 53BP1 focus formation is suppressed. (B) Quantification of data in A. At least 200 cells were counted for each treatment. Results depict the means

Table 1. **Fluorescence intensities of IR-induced nuclear foci**

Treatment	53BP1			γ-H2AX		
	Number of cells (*n*)	Foci per nucleus	Fluorescence intensity[a]	Number of cells (*n*)	Foci per nucleus	Fluorescence intensity[a]
			AU			*AU*
Control siRNA	2,377	26	4,100	2,501	22	1,588
RNF169 siRNA	1,351	25	6,127 (1.49×)[b]	1,343	19	1,685 (1.06×)[b]

U2OS cells treated with control or RNF169 siRNAs for 3 d were exposed to IR (0.25 Gy), fixed 30 min later, and immunostained with antibodies to 53BP1 or γ-H2AX. Numbers and intensity of IR-induced nuclear foci were quantified using ScanR image analysis software. Results from a representative experiment are shown. AU, arbitrary unit.
[a]The mean values of total fluorescence associated with all detectable IR-induced nuclear foci.
[b]Fold increase.

inhibitors and incubated on ice for 10 min, and lysates were cleared by centrifugation for 10 min at 20,000 rpm. Lysates were incubated with FLAG agarose (Sigma-Aldrich) or Strep-Tactin Sepharose (IBA BioTAGnology) for 1.5 h on an end-over-end rotator at 4°C, washed five times with EBC buffer or denaturing buffer, and resuspended in 2× Laemmli sample buffer. To analyze binding of RNF169 to ubiquitin chains, cells transfected with S-FLAG-Strep–tagged RNF169 constructs were lysed in denaturing buffer containing protease inhibitors and subjected to Strep-Tactin pull-down. Bound complexes were washed three times in denaturing buffer followed by two washes in EBC buffer and incubated with K48- or K63-linked polyubiquitin chains (Boston Biochem) for 2 h at 4°C. After thorough washing, immobilized material was resolved by SDS-PAGE and subjected to immunoblotting. For subcellular fractionation, the Subcellular Protein Fractionation kit (Thermo Fisher Scientific) was used according to the manufacturer's instructions. Rabbit polyclonal antibody to RNF169 (Eurogentec) was raised against the peptide RRSQPERCRPRRDGGA, corresponding to amino acids 134–149 in human RNF169, and affinity purified. Other antibodies used in this study included rabbit polyclonals to 53BP1, BRCA1, SP1, Cyclin A, HA (Santa Cruz Biotechnology, Inc.), Myc (Abcam), NF-κB–p65, histone H2A, and γ-H2AX (Cell Signaling Technology), mouse monoclonals to FLAG (Sigma-Aldrich), His_6 (Takara Bio Inc.), ubiquitin, and GFP (Santa Cruz Biotechnology, Inc.), conjugated ubiquitin (FK2; Enzo Life Sciences), Cyclin B (BD), and Plk1 (Invitrogen), and goat polyclonal to MCM6 (Santa Cruz Biotechnology, Inc.). Rabbit polyclonal antibodies to RNF168 and RAP80 were gifts from D. Durocher (Samuel Lunenfeld Research Institute, University of Toronto, Toronto, Ontario, Canada) and X. Yu (University of Michigan, Ann Arbor, MI), respectively. The sheep polyclonal MDC1 antibody was a gift from S. Jackson (Gurdon Institute, University of Cambridge, Cambridge, England, UK).

Immunofluorescence staining, microscopy, and laser microirradiation

For immunofluorescence staining, cells were fixed in 3% formaldehyde, permeabilized with PBS containing 0.2% Triton X-100 for 5 min, and incubated with primary antibodies diluted in DME for 1 h at room temperature. After staining with secondary antibodies (Alexa Fluor 488, 568, and 647; Life Technologies) for 30 min, coverslips were mounted in mounting medium (Vectashield; Vector Laboratories) containing nuclear stain DAPI. Images were acquired with a confocal microscope (LSM 710; Carl Zeiss) mounted on a confocal laser-scanning microscope (Axiovert 100M; Carl Zeiss) equipped with a Plan Apochromat 40×/1.3 NA oil immersion objective using standard settings: DAPI and Alexa Fluor 488/GFP, Alexa Fluor 568, and Alexa Fluor 647 dyes were excited with 405-, 488-, 546-, and 633-nm laser lines, and emitted light was collected through band pass 420–480-, 505–530-, and 560–615-nm and long pass 615-nm filters. Pinhole size was set to 1 airy unit or opened slightly for all wavelengths acquired if the signal intensity was otherwise too low. Image acquisition and analysis were performed with ZEN2010 software (Carl Zeiss). Raw images were exported as TIF files, and if adjustments in image contrast and brightness were applied, identical settings were used on all images of a given experiment. Laser microirradiation to generate local DSBs was performed as previously described (Lukas et al., 2003). In brief, cells grown on glass coverslips were treated for 24 h with 10 µM BrdU, placed in a 1-well dish (LabTek II; Thermo Fisher Scientific) containing prewarmed CO_2-independent medium (Life Technologies), and placed on the stage of a temperature-controlled (37°C) microscope (Axiovert 200M) with an integrated laser microbeam system (337-nm pulsed nitrogen laser; PALM Microbeam; Carl Zeiss). Using an LD Achroplan 40×/0.6 NA objective, the laser beam was focused to a 1-µm-wide track, and the proprietary PalmRobo software (Carl Zeiss) was used to place linear regions across nuclei for microirradiation. The energy output of the laser was chosen so that no DSBs were detected without BrdU sensitization, and the microirradiated area was strictly linear and confined locally. For each condition, ≥100 cells were microirradiated and fixed in 3% formaldehyde 1 h later.

Automated analysis of fluorescence intensities of nuclear foci

Exponentially growing U2OS cells were treated with control or RNF169 siRNAs (50-nM final concentration) for 3 d. Cells were then irradiated (0.25 Gy) and, 30 min later, fixed and immunostained with antibodies to 53BP1 or γ-H2AX. Each staining was performed in a separate imaging chamber, and in either case, the secondary antibody was coupled to Alexa Fluor 488 fluorophore to allow identical conditions for image acquisition and analysis. Nuclear DNA was counterstained with 0.25 mg/ml DAPI. A series of random fields were recorded automatically using the ScanR imaging workstation (Olympus; with an EM charge-coupled device camera [C9100; Hamamatsu Photonics], a U Plan S Apochromat 40×/0.9 NA objective, and an image resolution of 200 × 200 nm/pixel). The number and intensity of IR-induced nuclear foci were quantified using the ScanR image analysis software.

In vivo and in vitro ubiquitylation assays

In vivo and in vitro ubiquitylation assays were performed as previously described (Mailand et al., 2007). In brief, to assay histone H2A ubiquitylation in vivo, cells cotransfected with FLAG–histone H2A and Myc-tagged ubiquitin were lysed in denaturing buffer, subjected to FLAG immunoprecipitation, and analyzed by immunoblotting. For in vitro ubiquitylation assays, 1 µg histone H2A (New England Biolabs, Inc.) was incubated in 30 µl reaction mixture containing 50 mM Tris, pH 7.5, 5 mM $MgCl_2$, 2 mM NaF, 2 mM ATP, 10 µM okadaic acid, and 1 mM DTT supplemented with 0.1 µg E1, 0.2 µg UbcH5c, and 1 µg HA-ubiquitin (all obtained from Boston Biochem). 200 ng recombinant His_6-tagged full-length human RNF168 and/or RNF169 proteins purified from *Escherichia coli* by standard methods were added, and reactions were incubated for 1 h at 37°C, stopped by addition of Laemmli sample buffer, and resolved by SDS-PAGE.

(±SD) of three independent experiments. (C) U2OS cells transfected as in A were microlaser irradiated, fixed 1 h later, and coimmunostained with 53BP1 and RAP80 antibodies. (D) U2OS cells transfected and exposed to IR as in A were fixed and immunostained with the ubiquitin conjugate (FK2) antibody. (E) U2OS cells transfected with control (CTRL) or RNF169 siRNAs (see also Fig. S2 C) for 72 h were exposed to IR (1 Gy), fixed 30 min later, and processed for 53BP1 immunostaining. Representative images acquired with identical microscope settings are shown. (F) U2OS/DR-GFP cells were transfected with the indicated siRNAs for 48 h and then cotransfected with plasmids encoding I-SceI and RFP for 48 h. Flow cytometry analysis of the GFP/RFP ratio was used to measure HR efficiency. Data represent the means (±SD) of three independent experiments. (G) U2OS/DR-GFP cells were transfected with empty vector or RNF169 plasmids for 24 h and processed as in F. (H) Clonogenic survival of U2OS/S-FLAG-Strep–RNF169 WT cells induced or not induced with doxycycline (DOX) for 24 h and exposed to the indicated doses of IR. Results depict the means (±SD) of three replicates from one representative experiment. (I) As in H, using U2OS/S-FLAG-Strep–RNF169 *MIU cells. Expression of S-FLAG-Strep–RNF169 in cell lines is shown in Fig. S3 D. Bars, 10 µm.

Clonogenic survival assays

U2OS/S-FLAG-Strep–RNF169 WT, *MIU, or *RING cell lines were induced or not induced with doxycycline for 24 h, replated into 6-cm dishes, and allowed to adhere for 24 h before treatment with the indicated doses of IR. Cells were then incubated for an additional 10 d and stained with crystal violet. The resulting colonies containing >50 cells were scored as survivors. Results were corrected for plating efficiency.

HR and NHEJ assays

HR rates were assessed using a U2OS derivative cell line with an integrated HR reporter construct (direct repeat [DR]-GFP) essentially as previously described (Sartori et al., 2007). In brief, 2 d after transfection with siRNAs, U2OS/DR-GFP cells were cotransfected with plasmids expressing I-SceI, RFP, and, where indicated, empty vector or S-FLAG-Strep–RNF169. Transfection of RFP alone served as a reference for the absence of HR. Cells were collected 48 h after transfection and subjected to flow cytometric analysis to examine DSB-induced recombination. Only RFP-positive cells were analyzed for HR efficiency to circumvent possible differences in transfection efficiencies. Fluorescence-activated cell sorting data were processed using CellQuest software (BD) to determine the percentage of GFP-positive cells relative to the number of transfected cells (RFP positive). The dividing line between HR-positive and -negative cells were set to 1% background level of GFP-positive cells in the internal control (RFP positive, not transfected with I-SceI). This gate was subsequently applied to determine the HR efficiency in the RFP/I-SceI–positive samples. Analysis of NHEJ activity using an H1299dA3-1 reporter cell line (gift from T. Kohno, National Cancer Center Research Institute, Tokyo, Japan) was performed as previously described (Ogiwara et al., 2011). In brief, H1299dA3-1 cells were transfected with plasmids expressing I-SceI and S-FLAG-Strep–RNF169 or empty vector for 48 h and harvested. Where indicated, 20 µM DNA–protein kinase catalytic subunit inhibitor NU7026 (Sigma-Aldrich) was added to cells at the time of transfection. The proportion of GFP-positive cells (as a measure of NHEJ activity) was determined by flow cytometry.

Online supplemental material

Fig. S1 shows expression and subcellular localization of RNF169 during the cell cycle and in response to DNA damage. Fig. S2 shows impact of RNF169 overexpression and depletion on recruitment of DNA repair factors to sites of DNA damage. Fig. S3 shows effects of modulating RNF169 status on DSB repair and cell survival. Online supplemental material is available at http://www.jcb.org/cgi/content/full/jcb.201109100/DC1.

We thank Drs. Daniel Durocher, Xiaochun Yu, Takashi Kohno, and Stephen Jackson for providing reagents. We also thank Daniel Durocher for communicating results before publication.

This work was supported by grants from the Novo Nordisk Foundation, Danish Medical Research Council, the Danish Cancer Society, and the Lundbeck Foundation.

Submitted: 20 September 2011
Accepted: 7 March 2012

References

Acs, K., M.S. Luijsterburg, L. Ackermann, F.A. Salomons, T. Hoppe, and N.P. Dantuma. 2011. The AAA-ATPase VCP/p97 promotes 53BP1 recruitment by removing L3MBTL1 from DNA double-strand breaks. *Nat. Struct. Mol. Biol.* 18:1345–1350. http://dx.doi.org/10.1038/nsmb.2188

Bekker-Jensen, S., and N. Mailand. 2010. Assembly and function of DNA double-strand break repair foci in mammalian cells. *DNA Repair (Amst.)*. 9:1219–1228. http://dx.doi.org/10.1016/j.dnarep.2010.09.010

Bekker-Jensen, S., C. Lukas, R. Kitagawa, F. Melander, M.B. Kastan, J. Bartek, and J. Lukas. 2006. Spatial organization of the mammalian genome surveillance machinery in response to DNA strand breaks. *J. Cell Biol.* 173:195–206. http://dx.doi.org/10.1083/jcb.200510130

Bothmer, A., D.F. Robbiani, N. Feldhahn, A. Gazumyan, A. Nussenzweig, and M.C. Nussenzweig. 2010. 53BP1 regulates DNA resection and the choice between classical and alternative end joining during class switch recombination. *J. Exp. Med.* 207:855–865. http://dx.doi.org/10.1084/jem.20100244

Bouwman, P., A. Aly, J.M. Escandell, M. Pieterse, J. Bartkova, H. van der Gulden, S. Hiddingh, M. Thanasoula, A. Kulkarni, Q. Yang, et al. 2010. 53BP1 loss rescues BRCA1 deficiency and is associated with triple-negative and BRCA-mutated breast cancers. *Nat. Struct. Mol. Biol.* 17:688–695. http://dx.doi.org/10.1038/nsmb.1831

Bunting, S.F., E. Callén, N. Wong, H.T. Chen, F. Polato, A. Gunn, A. Bothmer, N. Feldhahn, O. Fernandez-Capetillo, L. Cao, et al. 2010. 53BP1 inhibits homologous recombination in Brca1-deficient cells by blocking resection of DNA breaks. *Cell*. 141:243–254. http://dx.doi.org/10.1016/j.cell.2010.03.012

Ciccia, A., and S.J. Elledge. 2010. The DNA damage response: making it safe to play with knives. *Mol. Cell*. 40:179–204. http://dx.doi.org/10.1016/j.molcel.2010.09.019

Coleman, K.A., and R.A. Greenberg. 2011. The BRCA1-RAP80 complex regulates DNA repair mechanism utilization by restricting end resection. *J. Biol. Chem.* 286:13669–13680. http://dx.doi.org/10.1074/jbc.M110.213728

Doil, C., N. Mailand, S. Bekker-Jensen, P. Menard, D.H. Larsen, R. Pepperkok, J. Ellenberg, S. Panier, D. Durocher, J. Bartek, et al. 2009. RNF168 binds and amplifies ubiquitin conjugates on damaged chromosomes to allow accumulation of repair proteins. *Cell*. 136:435–446. http://dx.doi.org/10.1016/j.cell.2008.12.041

Galanty, Y., R. Belotserkovskaya, J. Coates, S. Polo, K.M. Miller, and S.P. Jackson. 2009. Mammalian SUMO E3-ligases PIAS1 and PIAS4 promote responses to DNA double-strand breaks. *Nature*. 462:935–939. http://dx.doi.org/10.1038/nature08657

Hu, Y., R. Scully, B. Sobhian, A. Xie, E. Shestakova, and D.M. Livingston. 2011. RAP80-directed tuning of BRCA1 homologous recombination function at ionizing radiation-induced nuclear foci. *Genes Dev.* 25:685–700. http://dx.doi.org/10.1101/gad.2011011

Huen, M.S., R. Grant, I. Manke, K. Minn, X. Yu, M.B. Yaffe, and J. Chen. 2007. RNF8 transduces the DNA-damage signal via histone ubiquitylation and checkpoint protein assembly. *Cell*. 131:901–914. http://dx.doi.org/10.1016/j.cell.2007.09.041

Jackson, S.P., and J. Bartek. 2009. The DNA-damage response in human biology and disease. *Nature*. 461:1071–1078. http://dx.doi.org/10.1038/nature08467

Kim, H., J. Chen, and X. Yu. 2007. Ubiquitin-binding protein RAP80 mediates BRCA1-dependent DNA damage response. *Science*. 316:1202–1205. http://dx.doi.org/10.1126/science.1139621

Kolas, N.K., J.R. Chapman, S. Nakada, J. Ylanko, R. Chahwan, F.D. Sweeney, S. Panier, M. Mendez, J. Wildenhain, T.M. Thomson, et al. 2007. Orchestration of the DNA-damage response by the RNF8 ubiquitin ligase. *Science*. 318:1637–1640. http://dx.doi.org/10.1126/science.1150034

Lieber, M.R. 2008. The mechanism of human nonhomologous DNA end joining. *J. Biol. Chem.* 283:1–5. http://dx.doi.org/10.1074/jbc.R700039200

Lindahl, T., and D.E. Barnes. 2000. Repair of endogenous DNA damage. *Cold Spring Harb. Symp. Quant. Biol.* 65:127–133. http://dx.doi.org/10.1101/sqb.2000.65.127

Lukas, C., J. Falck, J. Bartkova, J. Bartek, and J. Lukas. 2003. Distinct spatiotemporal dynamics of mammalian checkpoint regulators induced by DNA damage. *Nat. Cell Biol.* 5:255–260. http://dx.doi.org/10.1038/ncb945

Mailand, N., S. Bekker-Jensen, J. Bartek, and J. Lukas. 2006. Destruction of Claspin by SCFbetaTrCP restrains Chk1 activation and facilitates recovery from genotoxic stress. *Mol. Cell*. 23:307–318. http://dx.doi.org/10.1016/j.molcel.2006.06.016

Mailand, N., S. Bekker-Jensen, H. Faustrup, F. Melander, J. Bartek, C. Lukas, and J. Lukas. 2007. RNF8 ubiquitylates histones at DNA double-strand breaks and promotes assembly of repair proteins. *Cell*. 131:887–900. http://dx.doi.org/10.1016/j.cell.2007.09.040

Misteli, T., and E. Soutoglou. 2009. The emerging role of nuclear architecture in DNA repair and genome maintenance. *Nat. Rev. Mol. Cell Biol.* 10:243–254. http://dx.doi.org/10.1038/nrm2651

Morris, J.R., C. Boutell, M. Keppler, R. Densham, D. Weekes, A. Alamshah, L. Butler, Y. Galanty, L. Pangon, T. Kiuchi, et al. 2009. The SUMO modification pathway is involved in the BRCA1 response to genotoxic stress. *Nature*. 462:886–890. http://dx.doi.org/10.1038/nature08593

Nakada, S., I. Tai, S. Panier, A. Al-Hakim, S. Iemura, Y.C. Juang, L. O'Donnell, A. Kumakubo, M. Munro, F. Sicheri, et al. 2010. Non-canonical inhibition of DNA damage-dependent ubiquitination by OTUB1. *Nature*. 466:941–946. http://dx.doi.org/10.1038/nature09297

Nicassio, F., N. Corrado, J.H. Vissers, L.B. Areces, S. Bergink, J.A. Marteijn, B. Geverts, A.B. Houtsmuller, W. Vermeulen, P.P. Di Fiore, and E. Citterio. 2007. Human USP3 is a chromatin modifier required for S phase progression and genome stability. *Curr. Biol.* 17:1972–1977. http://dx.doi.org/10.1016/j.cub.2007.10.034

Ogiwara, H., A. Ui, A. Otsuka, H. Satoh, I. Yokomi, S. Nakajima, A. Yasui, J. Yokota, and T. Kohno. 2011. Histone acetylation by CBP and p300 at double-strand break sites facilitates SWI/SNF chromatin remodeling and the recruitment of non-homologous end joining factors. *Oncogene*. 30:2135–2146. http://dx.doi.org/10.1038/onc.2010.592

Panier, S., and D. Durocher. 2009. Regulatory ubiquitylation in response to DNA double-strand breaks. *DNA Repair (Amst.)*. 8:436–443. http://dx.doi.org/10.1016/j.dnarep.2009.01.013

Penengo, L., M. Mapelli, A.G. Murachelli, S. Confalonieri, L. Magri, A. Musacchio, P.P. Di Fiore, S. Polo, and T.R. Schneider. 2006. Crystal structure of the ubiquitin binding domains of rabex-5 reveals two modes of interaction with ubiquitin. *Cell*. 124:1183–1195. http://dx.doi.org/10.1016/j.cell.2006.02.020

San Filippo, J., P. Sung, and H. Klein. 2008. Mechanism of eukaryotic homologous recombination. *Annu. Rev. Biochem.* 77:229–257. http://dx.doi.org/10.1146/annurev.biochem.77.061306.125255

Sartori, A.A., C. Lukas, J. Coates, M. Mistrik, S. Fu, J. Bartek, R. Baer, J. Lukas, and S.P. Jackson. 2007. Human CtIP promotes DNA end resection. *Nature*. 450:509–514. http://dx.doi.org/10.1038/nature06337

Shrivastav, M., L.P. De Haro, and J.A. Nickoloff. 2008. Regulation of DNA double-strand break repair pathway choice. *Cell Res.* 18:134–147. http://dx.doi.org/10.1038/cr.2007.111

Sobhian, B., G. Shao, D.R. Lilli, A.C. Culhane, L.A. Moreau, B. Xia, D.M. Livingston, and R.A. Greenberg. 2007. RAP80 targets BRCA1 to specific ubiquitin structures at DNA damage sites. *Science*. 316:1198–1202. http://dx.doi.org/10.1126/science.1139516

Sonoda, E., H. Hochegger, A. Saberi, Y. Taniguchi, and S. Takeda. 2006. Differential usage of non-homologous end-joining and homologous recombination in double strand break repair. *DNA Repair (Amst.)*. 5:1021–1029. http://dx.doi.org/10.1016/j.dnarep.2006.05.022

Stewart, G.S., S. Panier, K. Townsend, A.K. Al-Hakim, N.K. Kolas, E.S. Miller, S. Nakada, J. Ylanko, S. Olivarius, M. Mendez, et al. 2009. The RIDDLE syndrome protein mediates a ubiquitin-dependent signaling cascade at sites of DNA damage. *Cell*. 136:420–434. http://dx.doi.org/10.1016/j.cell.2008.12.042

Wang, B., S. Matsuoka, B.A. Ballif, D. Zhang, A. Smogorzewska, S.P. Gygi, and S.J. Elledge. 2007. Abraxas and RAP80 form a BRCA1 protein complex required for the DNA damage response. *Science*. 316:1194–1198. http://dx.doi.org/10.1126/science.1139476

Wu, J., M.S. Huen, L.Y. Lu, L. Ye, Y. Dou, M. Ljungman, J. Chen, and X. Yu. 2009. Histone ubiquitination associates with BRCA1-dependent DNA damage response. *Mol. Cell. Biol.* 29:849–860. http://dx.doi.org/10.1128/MCB.01302-08

Wyman, C., and R. Kanaar. 2006. DNA double-strand break repair: all's well that ends well. *Annu. Rev. Genet.* 40:363–383. http://dx.doi.org/10.1146/annurev.genet.40.110405.090451